NEW RESULTS FROM PETRA ON FRAGMENTATION AND NEUTRAL PARTICLES PRODUCTION

Daniel FOURNIER

Laboratoire de l'Accélérateur Linéaire
91405 ORSAY, FRANCE

ABSTRACT

New results on the neutral component of jets are presented, including first measurements of π° production. Then a short review is made of the description of multihadronic events by first order QCD and fragmentation models, and some differences between the Lund and Feynman-Field models are analyzed.

The last two parts of the talk are devoted to a review of correlations (including energy-energy correlations) and to some aspects of quark and gluon fragmentation.

CONTENTS

I. COMPARISON OF CHARGED AND NEUTRAL PARTICLE PRODUCTION

A large part of the results available up to now about multihadronic e^+e^- annihilation events were obtained mainly from charged particles. With the coming into operation of the high granularity liquid argon detectors of CELLO and TASSO, more detailed information about neutrals will become available. The first of these results are presented here.

1) Measurement of neutrals

The energy carried by neutral particles represents a large fraction (1) (about 38 %) of the total energy available in the final state of multihadronic events coming from e^+e^- annihilation at PETRA/PEP energies. Since most of the neutral energy is carried by photons (1), (2) the important devices to study the

neutral component of jets are electromagnetic calorimeters (a compilation (3) shows that the photonic energy fraction is almost constant - around 26 % - between 5 and 35 GeV).

However extracting clean information on neutrals from E.M. calorimeters is not easy, since about 1/3 of the total energy measured comes from charged particles interacting in the device (1).

Essentially two methods have been used :

Method 1 : The expected value of the energy lost by each charged particle is locally subtracted from the calorimeter signal. Remaining signals are grouped in neutral clusters (JADE (1), CELLO (2)).

Method 2 : A sophisticated "pattern recognition" procedure is used to identify photon showers (CELLO (2) , TASSO (4)). This procedure relies :

i) on investigating the lateral and longitudinal spread of each shower

ii) on geometrical linking between calorimeter showers and tracks reconstructed in the central detector.

Efficiencies and biases of both methods are controled by Monte-Carlo simulation. Method 1 has less granularity, but incorporates part of the signals due to K_L^o, n, $\bar{n}$. Also it's efficiency should be independant of the width of the hadron jets.

2) Flow of neutral energy

An analysis was performed by the CELLO group following a procedure initiated by MARK J (5) to study the flow of energy in multihadronic events.

The charged energy is obtained from measurements in the central tracking device, and the neutral energy from the liquid argon calorimeter using method 1.

Planar events are selected by a cut at 0.25 on the oblateness of the broad jet. Radiative and γ-γ events are eliminated by a cut at $0.5 * \sqrt{s}$ on the visible energy and at $|\cos\theta| > 0.5$ on the angle θ between the normal to the event plane and the beam axis.

The well known three bump structure is observed in the event plane when considering the overall energy flow (see fig. 1). The new information on this plot is that the neutral energy flow follows quite nicely the same shape, indicating that the neutral component is reminiscent of the same parton structure as the charged one is, and that the fragmentation effects are similar on both components. The ratio of neutral to total energy in the three bumps will be discussed in section IV.2.

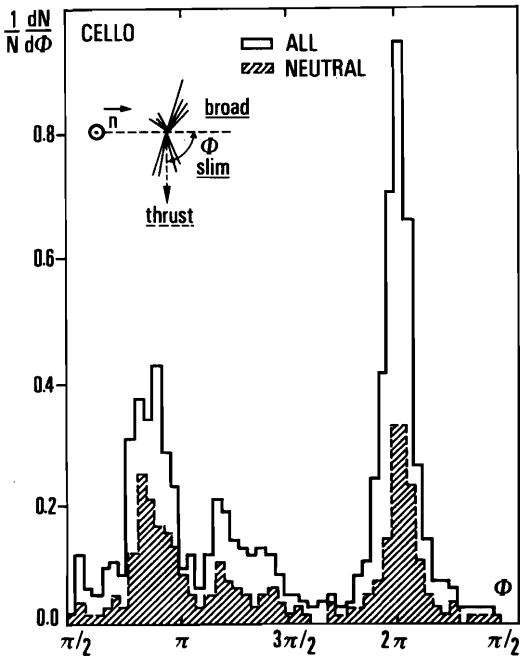

Fig. 1 : Energy flow and neutral energy flow at 36 GeV.

3) Properties of photons

Using method 2 the properties of photons were studied by the CELLO collaboration. A cut was made on the photon energy at 0.10 GeV.

The longitudinal and transverse momentum of photons with respect to the event thrust axis (determined using both the charged particles and photons) is shown in fig. 2.

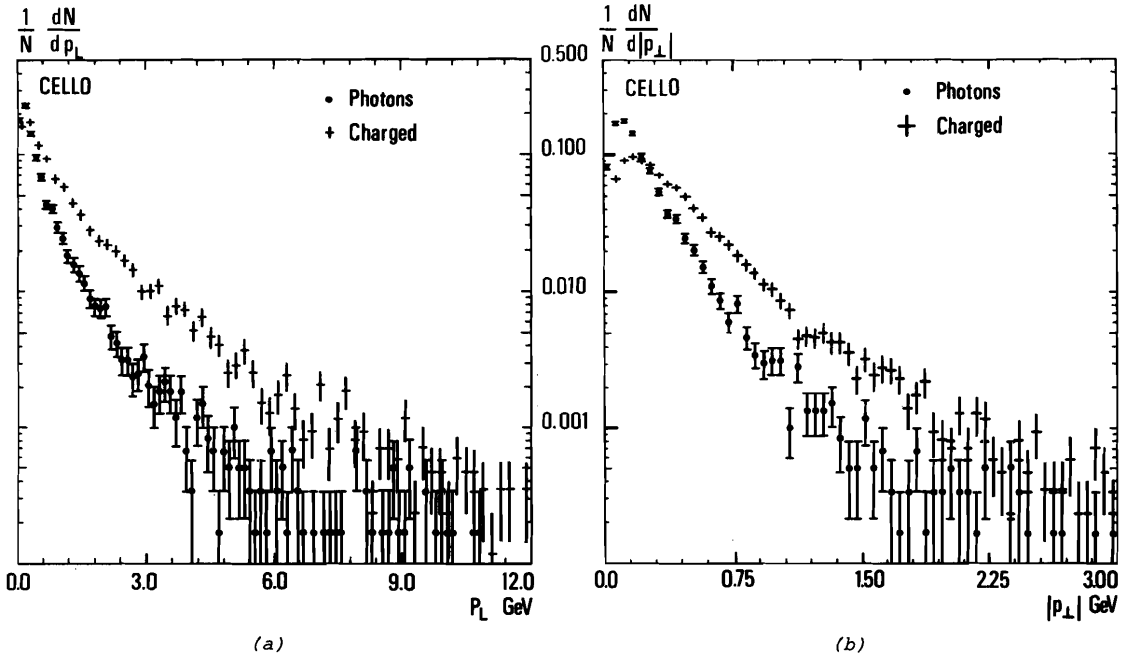

Fig. 2 : (a) Longitudinal and (b) transverse momentum of photons and charged particles (uncorrected data).

A Monte-Carlo simulation indicates that these spectra are not considerably distorted by the detector properties and by the reconstruction procedure. Since the same is true for charged particles, a comparison between charged and photon spectra on raw data may be relevant, at least at a semi-quantitative level.

One can see from fig. 2 that in the lower $p_\perp$ (1 GeV) and p_L (5 GeV) range the slope of the photon distribution is roughly twice larger than for charged particles. The same effect can be seen considering the mean values of $|p_\perp|$ and p_L. One gets 0.25 (0.47) GeV for the mean $|p_\perp|$ of neutrals (charged) and 0.65 (1.36) GeV for the mean p_L.

This contrasts with the similarity which is observed between the x distributions of various charged particles, and indicates that photons have undergone one more decay than the charged particles in the fragmentation process, as expected if they are dominantly from π° decay.

A thrust distribution of charged particles and photons with respect to the event thrust axis is shown in fig. 3. Again a close similarity is observed between charged particles and photons.

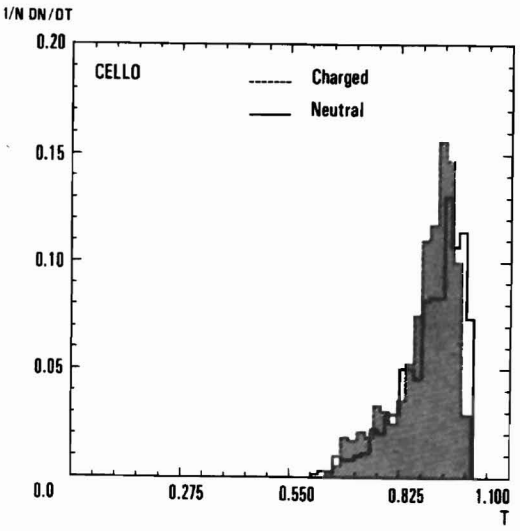

Fig. 3 : Thrust distribution of charged particles and photons (uncorrected data).

4) π° - reconstruction

Reconstruction of π° in multihadronic events was successfully achieved for the first time at PETRA by the TASSO collaboration.

Photons are reconstructed from the liquid argon data, and a π° signal is searched for, looking at the γγ invariant mass distribution. For that purpose a cut for better photon measurement is imposed at 0.15 GeV (low energy photons may loose a substantial fraction of their energy in the coil) and only those γγ combination for which the total (γ-γ) energy is between .5 and 4 GeV are considered (see below).

The γγ mass distribution (fig. 4.a) shows a clear π° peak centered at the right mass, over a background of wrong combinations. This background is well described by Monte-Carlo simulation, and can be statistically subtracted from the data. The curve obtained after subtraction (fig. 4.b) shows a nice π° peak with a width (σ) of about 25 MeV[1].

To obtain the π° energy spectrum, plots like 4.a and 4.b are made for the various γγ energy bins, and for each bin the number of π° is obtained by counting the number of events in the π° peak.

The efficiency of this π° reconstruction (including detector acceptance, ...) is estimated by following the same procedure with Monte-Carlo generated events. This shows that the efficiency drops considerably below .5 GeV (due to the photon energy cut) and above 4 GeV (due to the merging of the two photon showers).

The corrected momentum spectrum and x spectrum of the π° in that interval are shown in fig. 5.

A good agreement is observed between the π° spectra and the charged pion $(1/2(\pi^+ + \pi^-))$ spectra as expected from isospin invariance.

Conclusion

New results were presented on neutral energy flow, on photon spectra and on π° reconstruction and properties. The observed features are compatible with

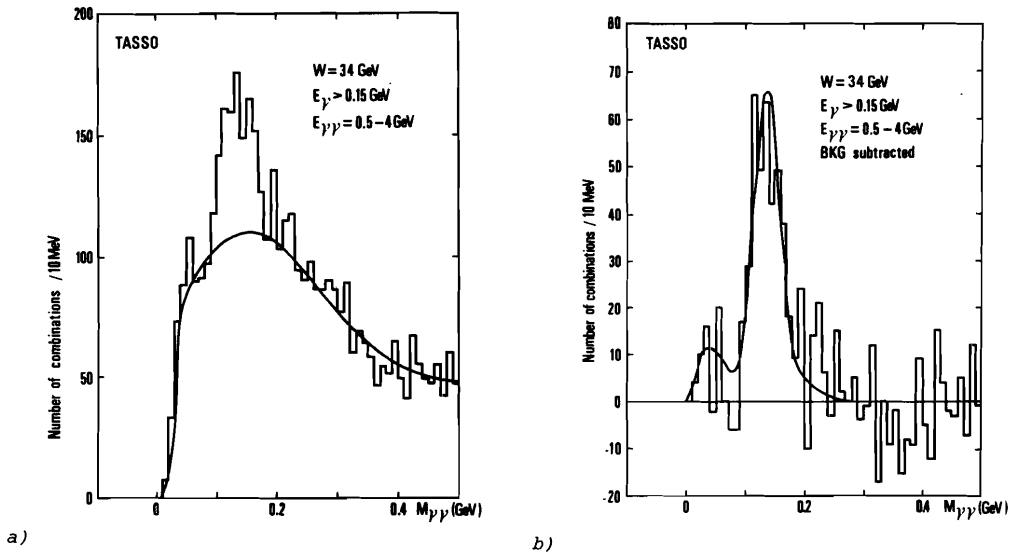

Fig. 4 : γγ mass spectrum
a) data - The curve is a Monte-Carlo estimate of the background
b) data after background subtraction.

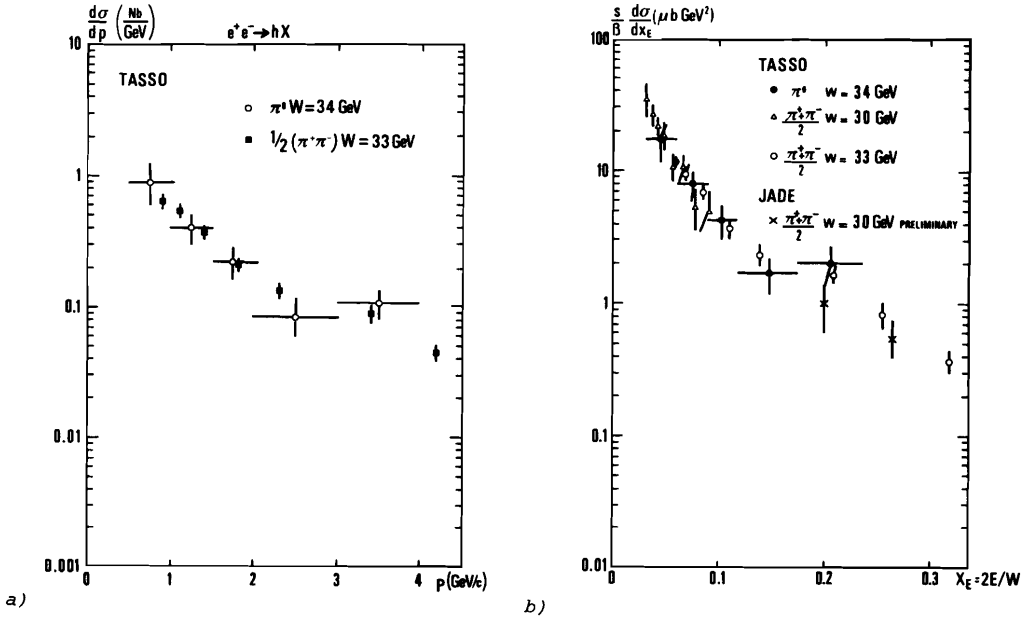

Fig. 5 : a) π° momentum spectrum
b) π° x spectrum

the π°'s being the dominant source of photons, and the measured x distribution of π° is similar to that of π^+ and π^-.

II. THE FRAGMENTATION PROCESS - MONTE-CARLO SIMULATIONS

Comparison of experimental data with theoretical predictions at the parton level requires simulation of fragmentation effects and detector properties.

Such simulations have shown that quite strong correlations exist between parameters at the parton level and some of the parameters of the fragmentation process (between α_S and σ_Q for example, see below).

It is therefore necessary to have a description as good as possible of the fragmentation process. Since no theory is presently available, phenomenological models have to be used.

It is important however to point out that the understanding of the transition between free partons to partons confined into hadrons is in itself of fundamental interest, and that the separation between (perturbative) phenomena at the parton level and the (non perturbative) fragmentation process is somewhat arbitrary.

The aim of this section is first to recall briefly which models are commonly being used, what are the main differences between them, and how well they describe the data in its gross features.

More subtle effects (correlations - differences between quark and gluon fragmentation) are reviewed in section III and IV.

1) The fragmentation models

The most extensively used Monte-Carlo simulations at PETRA at the present time are those from Hoyer et al. (6), Ali et al. (7) and from the Lund group (8).

In both simulations perturbative QCD effects at the parton level and fragmentation effects are treated independantly.

The first two simulations use the fragmentation model developped by Feynman and Field (9). A specific scheme based on the relativistic massless string model is used in the Lund simulation.

a) The Feynman-Field model

In this model each parton fragments independantly of the others. The fragmentation process is an independant cascade emission process. Starting from an energetic quark q of high W ($W = E + p_{/\!/}$) in a given reference frame, a quark-antiquark pair $q_1\bar{q}_1$ is generated in the colour field out of the vacuum. q and $\bar{q}_1$

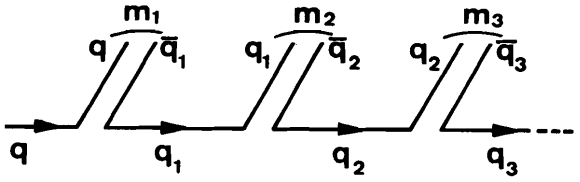

combine to form the first rank meson. This meson is given a fraction z of the W of the initial quark according to a distribution f(z). A quark q_1 is then left which in turn can trigger a new quark-antiquark pair creation out of the vacuum. The process stops when W reaches a threshold value W_0. The quarks leftout from the fragmentation of the various partons combine then to form the last hadrons.

Some specific features of the model as used in the simulations are the following :

- f(z) is given by $f(z) = 1 - a + 3a(1 - z)^2$ for light quarks
  $f(z) = 1$ for heavy quarks (c, b, ...)

- Each member of the $q_i\bar{q}_i$ pair is given a transverse momentum opposite to the other one. These momenta are then combined to give the meson transverse momenta.

  Quark transverse momenta are usually generated according to a gaussian law (of width σ_Q), but other laws, like exponential (10), have been suggested which are also compatible with the data (see report by W. Braunschweig at the same conference).

- Only light $q\bar{q}$ pairs are generated. A ratio $u\bar{u} : d\bar{d} : s\bar{s}$ like 2 : 2 : 1 is compatible with data (K production (11)).

- Only pseudoscalar (P) and vector mesons (V) are formed.

The main parameters of the model are therefore σ_Q, a, and P/(P + V). The gluon fragmentation is described by starting from the $g \to q\bar{q}$ conversion. The splitting of the energy between the two quarks can be made in different ways, for example according to the Altarelli-Parisi QCD prescription (12) $f(z) = z^2 + (1 - z)^2$ like in Ali et al. (7) ; or all of the energy can be given to only one quark, like in Hoyer et al. (6).

b) The Lund model

The Lund model, based on the massless string model, provides a relativistically invariant description of the fragmentation process. Like above, $q_i\bar{q}_i$ pairs are created out of the vacuum in the colour field, but the kinematics are different since the $q\bar{q}$ system, considered as a string, is treated as a whole and not as two independant objects.

At the expanse of somewhat more complicated kinematics, this seems to lead to a better rapidity plateau (8) and to better agreement with data as analyzed by the JADE collaboration (see § 3 below).

The fragmentation function preferred by the Lund group is $f(z) = (1 - z)^{\beta}$, but the Feynman-Field function can also be used.

The $q\bar{q}g$ events are treated as a string with a kink. This rely on the fact that similarities are found between colour forces in the $q\bar{q}g$ system and forces around the kink in the string model (13).

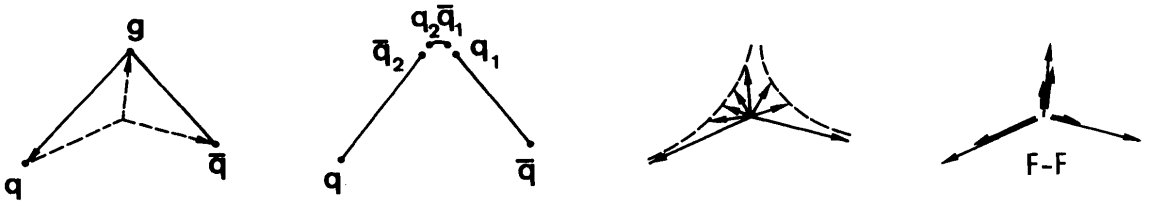

.The fragmentation process starts with the string being cut around the kink, giving rise to a $q_2\bar{q}_1$ meson and two strings $q\bar{q}_2$ and $q_1\bar{q}$.

The two strings then fragment independantly in their own center of mass frame, and the momenta in the overall center of mass system are then obtained by

the corresponding boost.

This scheme implies that, in the absence of transverse momenta in the fragmentation process, the extremity of the 3-momenta of final hadrons would lie, in the Lund scheme, on two hyperbolae, in contrast to the F.F. scheme where they would just lie along the initial parton momenta.

In the Lund model it is thus implied that a gluon jet will be softer than a quark jet with the same energy, but harder than just two quark jets with half the energy each.

First tests of these features will be shown in section IV.

2) Overall description of multihadronic events

Using data from 12 to 36 GeV, an overall determination of the parameters α_s, σ_Q, a and P/(P+V) was performed by the TASSO group (14) (using the simulation by Ali et al.).

The value obtained for the parameters are :

$\alpha_s = 0.17 \pm 0.02$ at 30 GeV (and $\alpha_s = 0.21$ at 12 GeV)

$\sigma_Q = 0.32 \pm 0.04$

$a = 0.57 \pm 0.20$

$P/(P+V) = 0.56 \pm 0.15$

Some of the errors are quite large due to important correlations essentially between a and P/(P+V) on one side and α_s and σ_Q on the other side. Fig. 6 shows that the agreement between the model and the data on sphericity, aplanarity and x distributions is quite good, both at low energy where the fragmentation effects

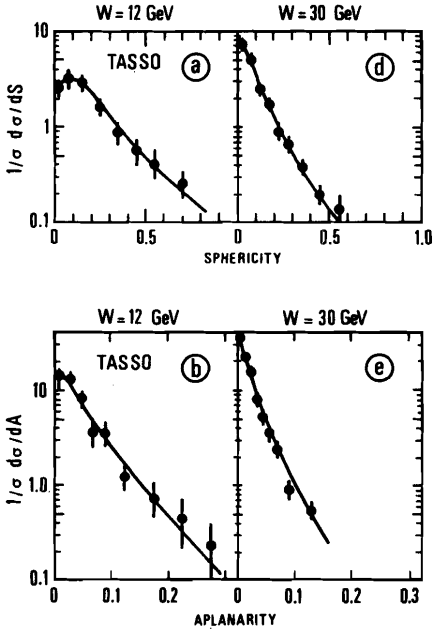

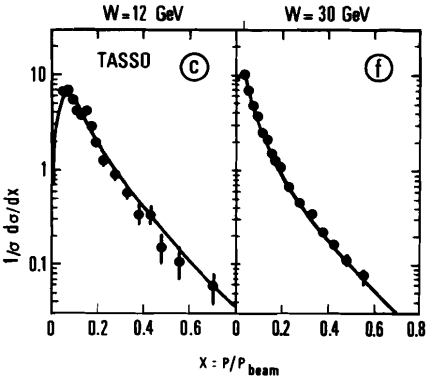

Fig. 6 : Sphericity, aplanarity and x distributions for 12 and 30 GeV data. Curves are Monte-Carlo distributions using parameter values quoted in the text.

are dominant and at high energy where hard gluon bremsstrahlung is important. Good agreement is also observed for the transverse momentum distribution in the event plane and out of the event plane. This is shown in fig. 7 where new data at 14,22 and 34 GeV is compared to calculations made using the values of the parameters quoted above.

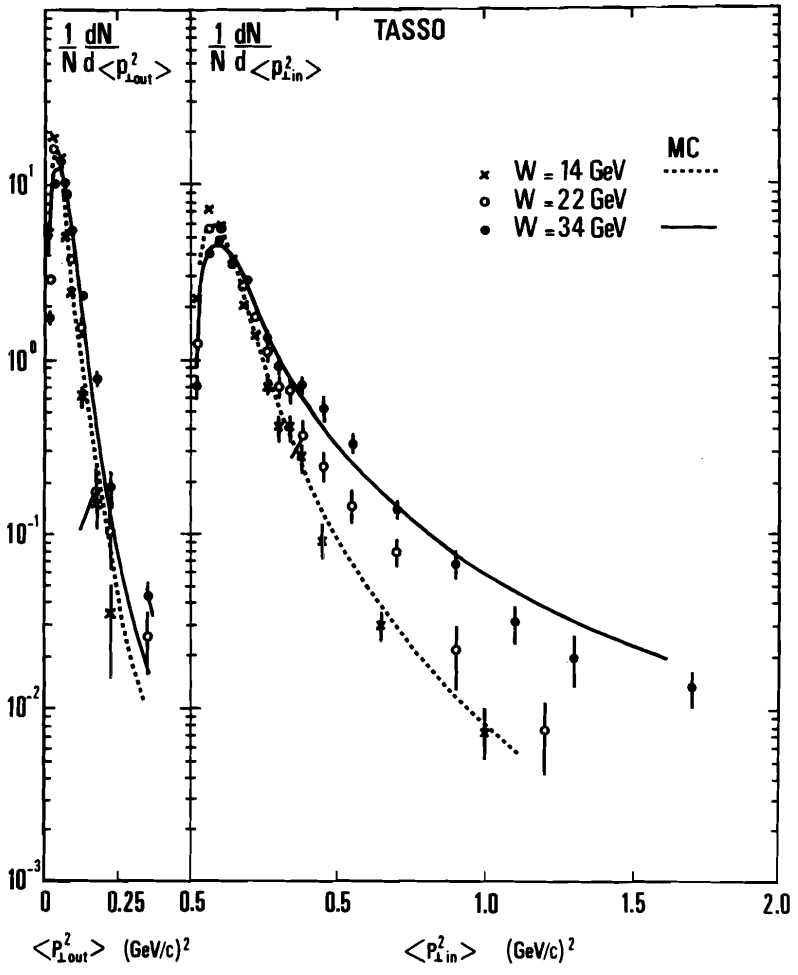

Fig. 7 : Distributions of transverse momentum out of the plane and in the plane for 14, 22 and 34 GeV data.

The observed correlation between α_s and σ_Q led to investigate fragmentation models where the transverse momentum distribution extends to values larger than for the gaussian distribution usually used. None of these models (5, 15) are able by themselves to fit the high energy data without including hard gluon bremsstrahlung. One may however guess that the systematic error on α_s might be larger than the values usually quoted ($\simeq$ 0.03) in the framework of fragmentation models using gaussian distributions.

3) Some specific features of the fragmentation models

a) Heavy quark fragmentation and heavy meson decay

The fragmentation function of heavy quarks is usually taken uniform. This means that heavy mesons should carry a higher fraction of the initial quark energy than light first rank mesons (cf. § 1.a). This can be investigated by looking at the inclusive momentum distribution of muons observed in multihadronic annihilation events. Measurements from MARK J have shown (cf. fig. 8.a) that even at high momentum where decays from B-mesons dominate, the agreement between data and Monte Carlo simulation (Ali et al.) is very good. The momentum transverse to the jet axis, which is essentially sensitive to the heavy meson decay process, is also well reproduced by the same Monte-Carlo calculation (fig. 8.b).

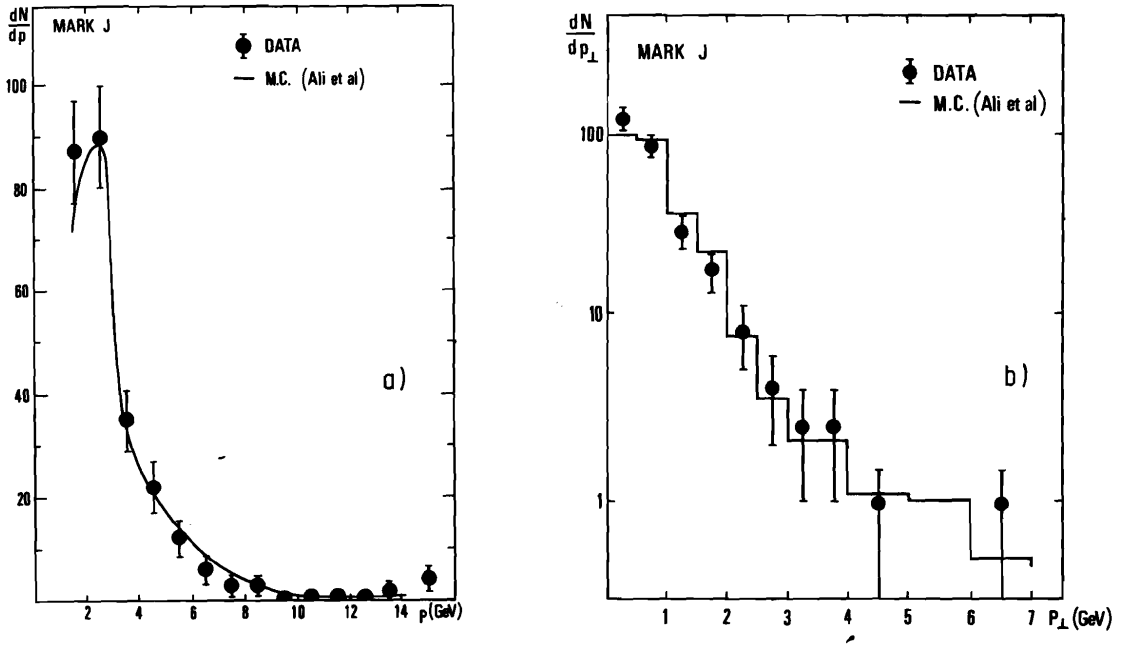

Fig. 8 : Inclusive distribution of muons a) momentum, b) momentum transverse to the jet axis.

b) Test of the fragmentation scheme

An investigation of the fragmentation scheme (Lund or Feynman-Field) was made by the JADE group, looking at the distribution of a quantity sensitive to the fragmentation near z = 1. The quantity used, η, is the mean value of cos θ_i (taken for particles belonging to the slim jet), where θ_i is the angle between the momentum of particle i and the sphericity axis.

The distribution obtained for η is shown in fig. 9 together with Monte-Carlo simulations following the Lund scheme and the Feynman-Field scheme (Hoyer et al. (6)) both using the same fragmentation function $f(z) = 1 - a + 3a(1 - z)^2$. One sees that the Lund scheme gives better agreement with data, and that agreement of the Feynman-Field simulation with data is not likely to be improved by changing the value of a, since discrepancies are observed at both ends of the spectrum.

A simulation with the Lund model using $f(z) = (1 - z)^2$ (not shown) gives still better agreement with the data, the small deviation for $z \to 1$ having disappeared.

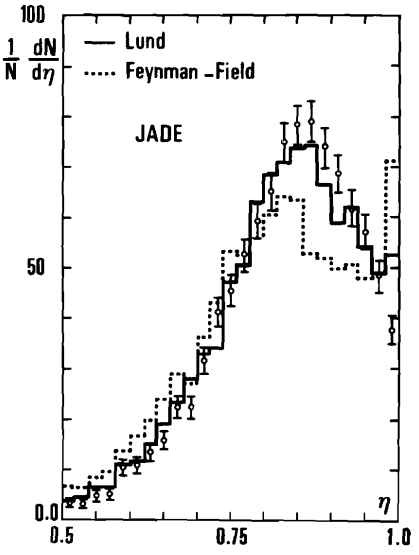

Fig. 9 : Distribution of η. The histograms are Monte-Carlo calculations made with $f(z) = 1 - a + 3a(1 - z)^2$ [$a = 0.50$].

To conclude, both models, when combined with hard gluon bremsstrahlung, are able to give a good overall description of the data. But on a specific point concerning the z distribution, the string model in which the $q\bar{q}$ system is considered as a whole, seems to have some superiority over the Feynman-Field model.

III. CORRELATIONS

Various kinds of correlations between hadrons formed during the fragmentation process have been investigated. Rapidity correlations and charge correlations are sensitive to the existence of intermediate clusters, while baryon-baryon correlations may give some insight into the baryon formation mechanism.

Energy-energy correlations play a special role since they are sensitive both to soft (hadronisation) and hard (parton emission) processes.

1) Charge and rapidity correlations

a) Rapidity correlations

Rapidity along the event sphericity axis is defined as $y = \frac{1}{2} \text{Log}\ ((E + P_L)/(E - P_L))$. The single particle density is estimated by computing $\rho_1(y) = \frac{1}{\Delta y} < \sum_i \delta_{iy} >$ where <> means the mean value over a sample of N events. In the same way $\rho_2(y,y') = \frac{1}{\Delta y \Delta y'} < \sum_k \sum_{i \neq k} \delta_{iy}\, \delta_{ky'} >$ represents the combined probability per unit y interval that a particle is produced at y together with another one at y'. The "associated two particle density" $\rho'(y,y') = \rho_2(y,y')/\rho(y')$ (which is the probability that if a particle is produced at y' another one is

also produced at y), is shown in fig. 10 as a function of y for different bins

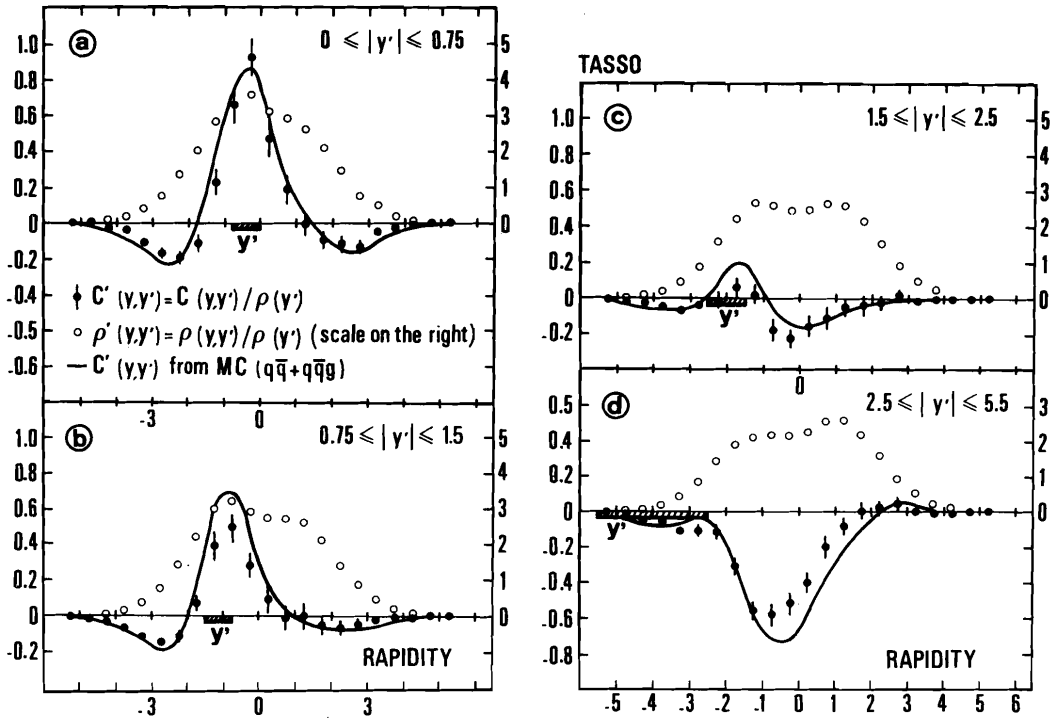

Fig. 10 : Associated two particle density ρ'(y,y') and correlation C'(y,y') as a function of y for different selected bins of y'. The curves are the result of a Monte-Carlo simulation.

in y'. One sees that ρ'(y/y') has a tendancy to peak around y = y' (at least in the plateau region $|y'| \lesssim 2.5$) indicating a positive short range correlation. This is better seen by looking at the "associated two particle correlation"

$$C'(y,y') = \frac{1}{\rho(y')} \{\rho_2(y,y') - \rho(y)\ \rho(y')\}$$

which is plotted in fig. 10 together with ρ_2 (data from TASSO).

These short range rapidity correlations show the role played by intermediate clusters (resonances) in the fragmentation process. The Monte-Carlo simulation (Ali et al.) reproduces quite well the observed correlations, both in width and strength, except perhaps for the large y' values where some deviation may be seen. One could tentatively associate this observation with the problems encountered with the Feynman-Field model in the large x region (cf. § II.3).

The observed correlations are similar in width but somewhat stronger than the correlations observed in the central rapidity region of p-p collisions at similar energy (17) (ISR data). This feature might be understood if one views pp collisions in the central area as overlapping jets (18).

b) Charge correlations (19)

The mechanism of charge compensation in rapidity space can be investigated by looking at the difference between positive and negative two particle density when, for example, a negatively charged particle is observed between y' and y' + Δy'. In order to do that, one defines :

$$\Phi(y,y') = \rho^{+-}(y,y') - \rho^{--}(y,y') + \rho^{-+}(y,y') - \rho^{++}(y,y')$$

$$\Phi(y,y') = -\frac{1}{\Delta y \Delta y'} \left\langle \sum_{k=1}^{n} e_k \, \delta_{ky'} \sum_{i \neq k} e_i \, \delta_{iy} \right\rangle$$

and the charge compensation probability (or normalized reduced charge flow) :

$$\tilde{\Phi}_r(y,y') = \frac{1}{\rho(y')} \cdot \frac{-1}{\Delta y \Delta y'} \left\langle \frac{1}{n} \sum_{k=1}^{n} e_k \, \delta_{ky'} \sum_{i \neq k} e_i \, \delta_{iy} \right\rangle$$

e_i is the charge of particle i, n is the event multiplicity, and $\rho^{ij}(y,y')$ is the two particle density with a particle of charge j at y' and a particle of charge i at y.

The results obtained by the TASSO collaboration are shown in fig. 11.

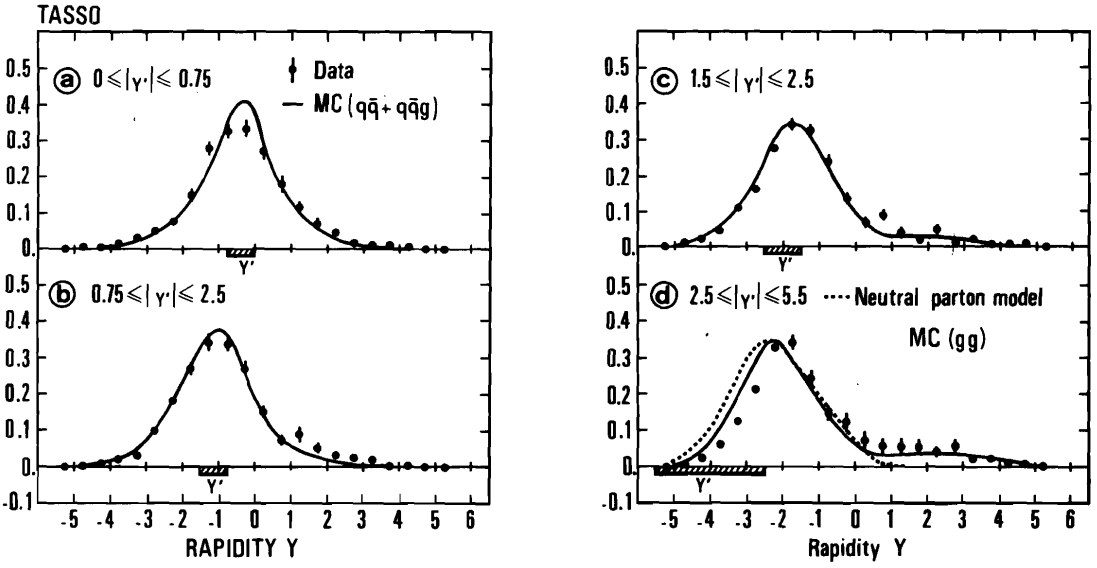

Fig. 11 : Normalized reduced charge flow $\tilde{\Phi}_r(y,y')$ as a function of y for different selected bins of y'.

A clear short range correlation is observed indicating a large dominance of local charge compensation. The charge correlation length observed (≃ 1 rapidity unit for $\langle |y - y'| \rangle$) is very close to the value observed in proton-proton collisions (17).

Beside the main effect of local charge compensation, a long range charge compensation effect is also observed for $|y'| \gtrsim 2.5$. Both effects are well described by a ($q\bar{q}$ + $q\bar{q}g$) Monte-Carlo simulation, but a "neutral parton" model fails to reproduce the long range correlation.

This long range correlation shows that the fast particles in one jet know about the charges of the fast particles in the other jet, which can be considered as an evidence that primary partons carry an electric charge.

Short range correlations, which are naturally explained in terms of resonance formation and decay, are well described by Monte-Carlo simulations which incorporate these features.

2) Baryon-antibaryon correlations

First results on baryon production at PETRA became available recently (20,21). Two important features were observed :

i) the baryon-antibaryon yield is relatively high (each event contains an average of about 0.5 baryon-antibaryon pair)

and ii) the x dependence of the baryons is similar to that of K mesons (21), i.e. the baryon to meson ratio, if not constant, probably rises with x.

In a way similar to that leading to mesons (cf. § II.1) baryons can be formed in the fragmentation process from color triplet diquark - antidiquark pairs created out of the vacuum.

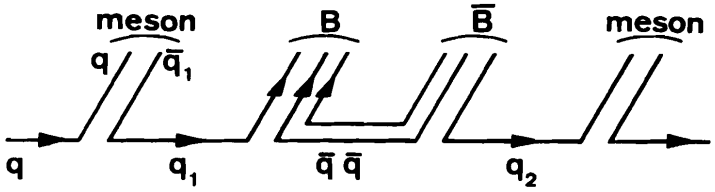

Such a model predicts an x distribution of baryons similar to that of mesons, and between baryon-antibaryon pairs, a short range rapidity correlation and a local compensation of the transverse momentum.

This model was incorporated in the above mentioned Monte-Carlo simulations and gives a reasonable estimate of the observed x spectra (22,23). Models giving rise to leading baryon effects in opposite jets have also been considered (22,24). The accuracy of present measurements is not good enough to estimate the contribution of such mechanisms.

A first test on baryon-antibaryon correlations was made by the JADE collaboration. Out of a sample of 400 events with one antiproton between .3 and .9 GeV/c, 12 events were found containing also a proton in the same momentum range[2]. Due to the momentum cut, the rapidity interval between the two baryons is limited to a maximum value of 1.5 rapidity unit. It is therefore interesting, in the framework of the model mentioned above, to look for local transverse momentum conservation. This was done by looking at the angle Φ between the momenta of the two particles projected onto the plane normal to the sphericity axis. Fig. 12 shows that the values of Φ are clustering between $\pi/2$ and π, thus indicating a local $P_\perp$ balance for baryon-antibaryon pairs close in rapidity.

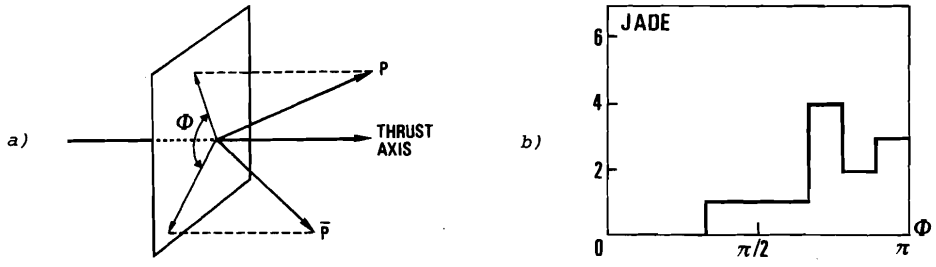

Fig. 12 : Baryon-antibaryon correlation - a) kinematic configuration b) Φ distribution.

3) Energy-energy correlations

a) Definition and properties

The energy-energy correlation is a distribution of the angles between all particles of the final state, weighted by the energy of these particles ($z_{a,b}$ is the energy of particle a, b relative to the beam energy):

$$f(\theta) = \frac{1}{\sigma}\frac{d\sigma}{d\theta} = \frac{1}{\sigma}\sum_{a,b}\int z_a z_b \frac{d\sigma}{dz_a\, dz_b\, d\theta}\, dz_a\, dz_b \quad .$$

$f(\theta)$ is measured by computing on a sample of N events.

$$f(\theta) = \frac{2}{N\Delta\theta}\sum_{N}\sum_{\text{pairs in } \Delta\theta} z_a\, z_b \quad .$$

For $\theta \to 0$ or $(\pi - \theta) \to 0$, $f(\theta)$ should be dominated by soft hadronisation effects. However for θ fixed not too small, $f(\theta)$ is sensitive to hard processes, due to the energy weighting, and energy-energy correlations have been proposed as sensitive tests of QCD.

First results were obtained by the PLUTO collaboration (29), and new data with larger statistics were presented at this conference by the CELLO collaboration.

Three regions of θ should be distinguished, in which $f(\theta)$ can be calculated within different approximations.

b) The central region ($30° \lesssim \theta \lesssim 150°$)

The main contribution to $f(\theta)$ in this region should be from single gluon bremsstrahlung. Calculations were made to the first order in α_s by Basham, Brown Ellis and Love (BBEL (25)) who show, among other interesting features, that $f_{QCD}(\theta)$ is proportional to α_s and that $f_{QCD}(\theta)$ is asymmetric around $\theta = 90°$.

Before any comparison with the data, this first order calculation should be modified to include non (QCD) radiative $q\bar{q}$ events contributing also in that area due to fragmentation effects. A simple, limited $P_\perp$ model (25) shows that $f_{FRAG}(\theta)$ is symmetric around $\theta = \pi/2$ and can be written $f_{FRAG}(\theta) = C \langle P_\perp \rangle / \sin\theta \sqrt{s}$.

The measured distribution $f(\theta)$, corrected for radiative effects in the initial state and for detector acceptance and resolution, is shown in fig. 13.a, together with the absolute QCD prediction (dashed curve, $\alpha_s = .14$), and a best fit of $f_{QCD}(\theta) + f_{FRAG}(\theta)$ with C as a free parameter.

One sees that at this energy (34 GeV) QCD effects and fragmentation effects give about equal contributions in the central area. The asymmetry characteristic of single hard processes is however clearly visible, and amounts to about 40 % between 40° and 140°.

Since the fragmentation contribution is symmetric around 90°, and the QCD contribution is not, one can think of isolating the hard process by looking at $f(\pi-\theta) - f(\theta)$. Data obtained in this way are shown in fig. 13 b.

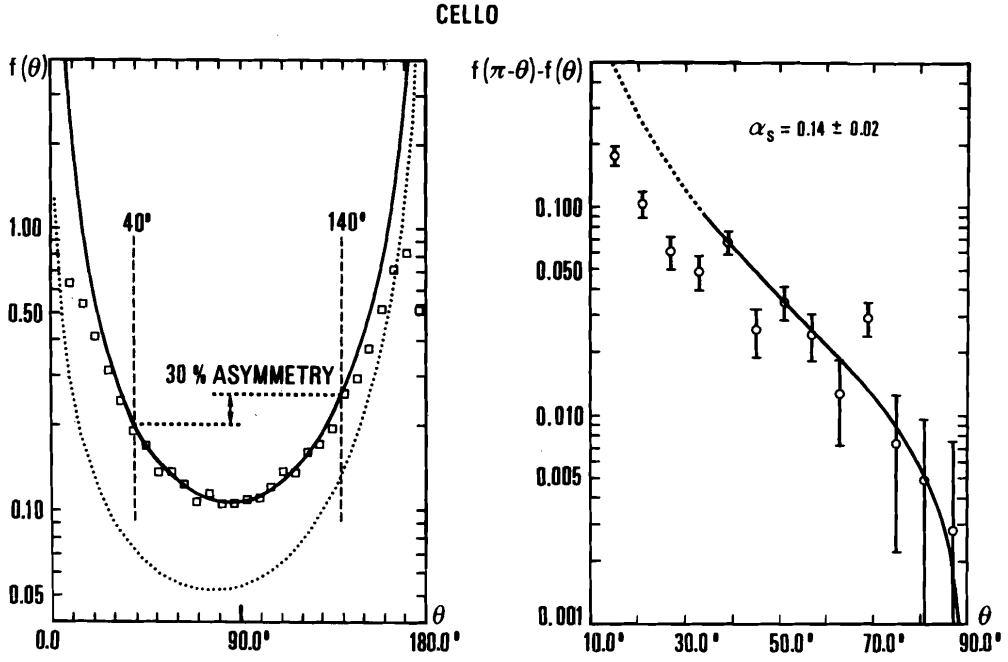

Fig. 13 : Energy-energy correlation at 34 GeV.
a) f(θ) - corrected data. The dotted curve is a first order QCD calculation (25) with α_s = .14. The full curve includes fragmentation effects.
b) f(π - θ) - f(θ). The full curve is a first order QCD calculation with α_s = .14

A best fit to the CELLO data (between 36° and 90°) of $f_{QCD}(\theta)$ with α_s as a free parameter gives $\alpha_s = 0.14 \pm 0.02$ (statistical) ± 0.02 (systematic) at 34 GeV.

c) The forward and backward regions

For θ small, f(θ) measures the jet opening angle and is sensitive to the radiation of real soft gluons and the cascading of virtual partons. Calculations to all orders of $\alpha_s(q^2)/\pi . \mathrm{Log}(Q^2/q^2)$ ($q^2 \simeq Q^2\theta^2$) have been performed in the leading logarithms approximation (LLA) by Konishi, Ukawa and Veneziano (26). The domain of validity of these calculations is restricted to $\Lambda^2/Q^2 << \theta^2 << 1$.

Similarly, for π-θ small ($\Lambda^2/Q^2 << (\pi-\theta)^2 << 1$), the dominant terms are those in $\alpha_s(q^2)/\pi . \mathrm{Log}^2(Q^2/q^2)$ ($q^2 \simeq Q^2(\pi-\theta)^2$). Calculations to all orders in the leading double logarithms approximation have been performed by several groups (27, 28).

In fig 14 the (uncorrected) distribution f(θ) obtained by the CELLO collaboration at 34 GeV is shown, compared first with a Monte-Carlo simulation (Ali et al.) including QCD effects to the first order (α_s = .16), the fragmentation being treated in the Feynman-Field model (cf. § II.1). One sees that the agreement between data and simulation is quite good over the whole range of θ, and one can wonder if there is any contribution to the data of high order processes.

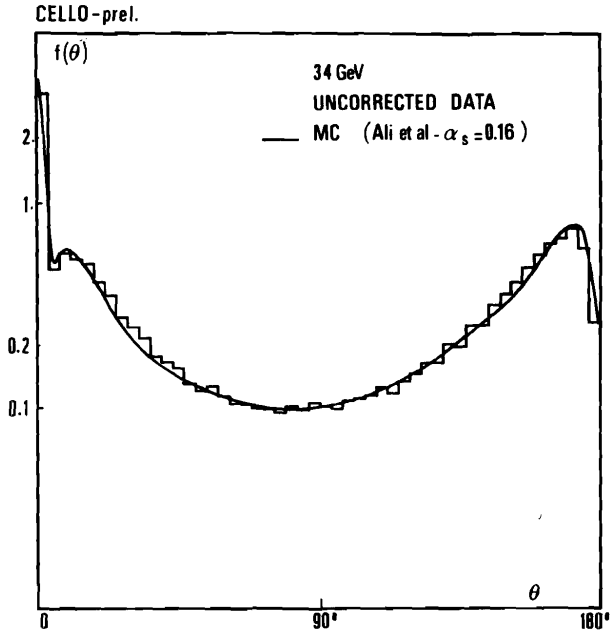

Fig. 14 : Energy-energy correlation at 34 GeV. The histogramm is the uncorrected data. The full curve is a Monte-Carlo simulation (Ali et al., α_s = .16)

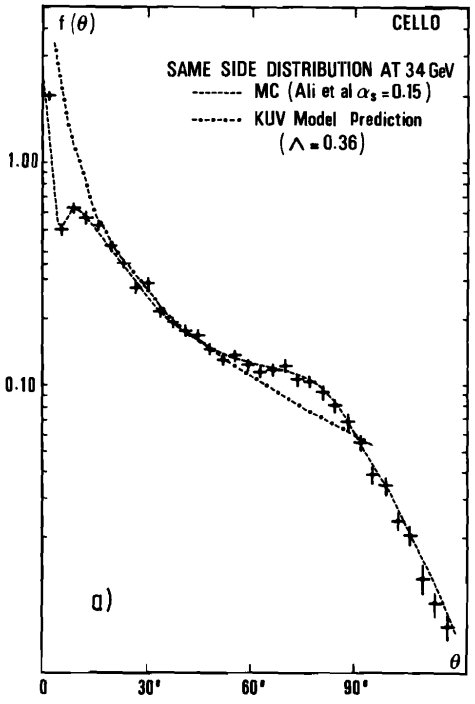

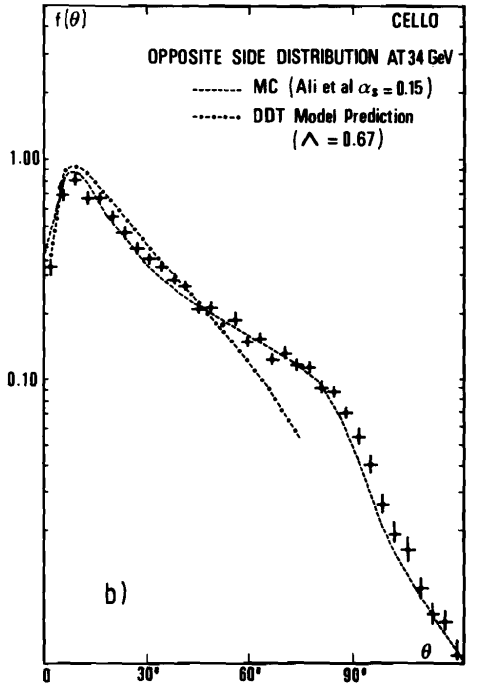

Fig. 15 : a) Same side energy correlations. Corrected data Curves are absolute QCD predictions from KUV (26).

b) Opposite side energy correlations. Corrected data. Curves are absolute QCD predictions from D.D.T. (27).

The energy correlation distribution $F_s(\theta)$ obtained by computing $f(\theta)$ only for those pairs which lie on the same side of a plane normal to the event thrust axis is shown in fig. 15.a, together with the absolute QCD predictions of KUV (26). The calculation does not really fit the data down to small angles, but a reasonable agreement is obtained in the range $15° \lesssim \theta \lesssim 60°$ for $\Lambda = 0.36$. A similar work done at 22 GeV (not shown) shows that the agreement between data and theory significantly improves between 22 and 34 GeV.

In a similar way $F_0(\theta)$ is obtained by computing $f(\theta)$ only for those pairs which lie on opposite sides of a plane normal to the event thrust axis. Data at 34 GeV are shown in fig. 15.b together with the absolute prediction of DDT (27). The agreement obtained is only qualitative, and worse than for the same side distributions. It was pointed out however (30) that calculations by Baier and Fey (29) should represent an improvement to the work of DDT and might be in better agreement with the data.

The important point to notice is that, although first order QCD and fragmentation models give a good description of the data, other descriptions seem to become possible which rely more deeply on QCD calculations.

This led to an other approach for Monte-Carlo simulations : fragmentation is taken as simple as possible (isotropic decay) but the QCD cascade is generated down to small masses ($\simeq$ 1 GeV) using the "jet calculus" (26) based on leading logarithms approximation. Such an approach is presently being carried out by various authors like Field (31), Fox and Wolfram (32) and Odorico et al. (33).

IV. QUARK AND GLUON FRAGMENTATION

Most of the results considered in the two preceding sections concerned essentially quark jets. It would however be of great interest to be able to compare quark jets and gluon jets of similar energies.

Some important results were obtained by comparing events produced on top of the Υ resonance with events from the nearby continuum (34) ; but, in most respects, the Υ mass is too low to allow a good separation of the three gluon jets, and therefore a detailed study of their properties.

The three jet events produced at the highest PETRA energies are an alternate source of gluon jets, from which some new results were obtained recently.

1) General properties of gluon fragmentation

From QCD one expects that, because the three gluon coupling is larger than the $q\bar{q}g$ coupling, gluon jets should be broader than quark jets. Calculations in the leading logarithms approximation show for example that, at asymptotic energies, the jet opening angles are expected to be in the ratio 9/4 (26), as is also expected to be the ratio of the multiplicities (35).

Various methods can be applied to identify the gluon jet in planar events considered as three jet event candidates. One of these methods consists in finding the grouping of particles in three jets, and the jet directions, in such a way that the generalized thrust, or triplicity, be maximized (36). From the three angles θ_1, θ_2, θ_3 between the jet directions ($\theta_1 < \theta_2 < \theta_3$) one then calculates the three energies E_1, E_2, E_3 ($E_1 > E_2 > E_3$). The jet with the smallest energy is then called the gluon jet (see fig. 17). According to a Monte-Carlo simulation (16), 51 % of the jets selected in this way are genuine gluon jets, while jet 2 and jet 1 are respectively in 22 % and 12 % of the cases originating from gluons.

A study of the transverse momentum distribution of particles with respect to the jet axis determined in this way was carried out by the JADE collaboration. This study, which was also reviewed in the talk by W. Braunschweig (15), shows the following features :

- the mean transverse momentum of particles in the gluon jet (jet 3) is slightly larger than for quark jets of the same energy (see fig. 16).

- the broadening is more important in the event plane than normally to the event plane.

- both features are quite well reproduced by the Lund Monte-Carlo simulation, while they are not reproduced by the Hoyer et al. simulation in which quark and gluon fragment in the same way (see § II.1).

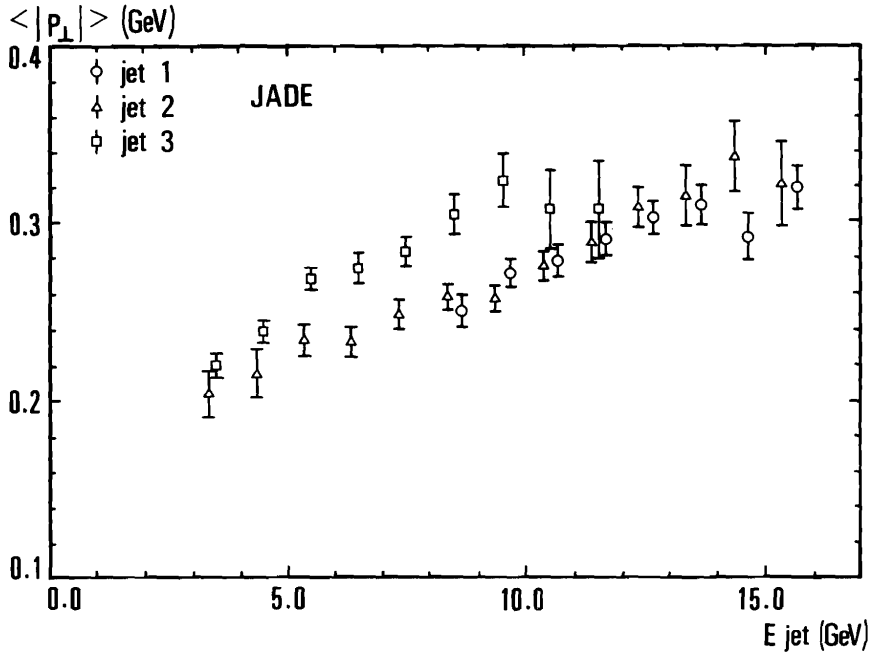

Fig. 16 : Mean transverse momentum of particles in each of the three jets of a planar event, as a function of the jet energy.

To the extent that the observed features can be considered as a success of the string model, it is worthwhile looking at other phenomena which might be considered as specific of this model.

One of those is the particle angular distribution in the event plane (16), for which some new data were presented by the JADE collaboration.

The average number of charged and neutral particles per event is plotted in fig. 18 as a function of the normalized projected angle φ_i/θ_i.

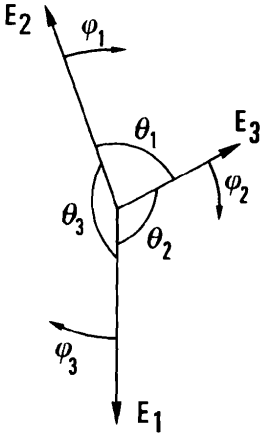

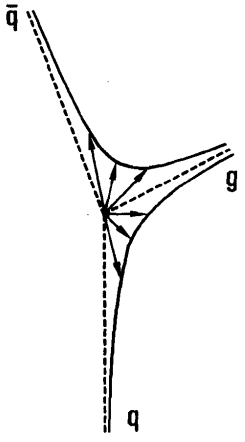

Fig. 17 : Kinematics of three jet events

One observes that the particle density is significantly smaller between the q and the $\bar{q}$ than between the gluon and the quark or antiquark. Here again a good description is provided by the Lund string model, while the model of Hoyer et al. fails to reproduce this specific feature.

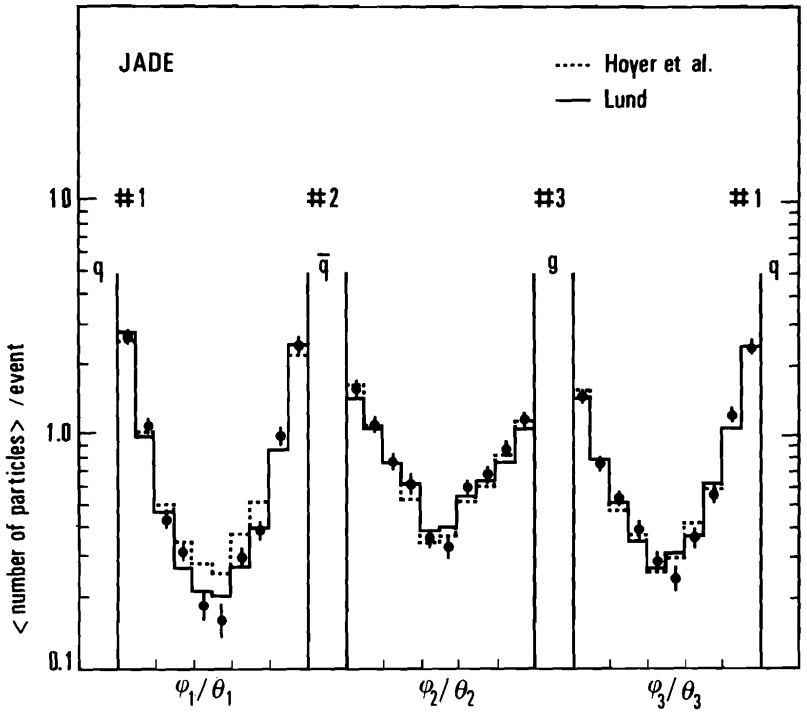

Fig. 18 : Mean number of particles as a function of the normalized angle.

Since in the Lund model, the observed phenomena are associated to the Lorentz boost from each string subsystem to the overall center of mass system (see § II.1 and Fig. 17) they should be more pronounced for particles with larger mass or larger momentum transverse to the event plane (P_{out}). This effect was estimated (16) by taking the ratio of the number of particles in the central area between jet 1 and 3 ($.3 < \varphi_1/\theta_1 < .7$) to the corresponding number for jets 1 and 2. The observed ratio R are listed in table I.

	Particles	Data	Models	
			Lund	Hoyer et al.
R	all	1.35 ± 0.07	1.34 ± .06	1.08 ± .04
	P_{out} < 0.2 GeV	1.25 ± 0.09	1.29 ± .07	1.02 ± .05
	P_{out} > 0.2 GeV	1.55 ± 0.18	1.43 ± .12	1.20 ± .09
	K mesons	2.3 ± .5	1.74 ± .4	.89 ± .20

Table I

In spite of the limited statistics, the data do exhibit an increase of the asymmetry with increasing m^2 or P^2_{out}, and again a better agreement is observed with the Lund model than with the Höyer et al. simulation which uses the Feynman-Field model with the same fragmentation functions for quarks and gluons.

2) Particle content of quark and gluon jets

a) Fraction of energy carried by photons

Working on the particle content of gluon jets, Peterson and Walsh (37) proposed a scheme of gluon fragmentation in which isoscalar particles play a dominant role ; according to the relative contributions of η and η' this may lead to an excess of photonic energy in gluon jets compared to quark jets.

A measurement of the ratio of photonic energy to charged energy in jets 1, 2 and 3 of planar events (cf. § IV.1) was performed by the JADE collaboration (1). The values they obtained were 0.47 ± 0.01, 0.46 ± 0.01 and 0.44 ± 0.02 in jets 1, 2 and 3 respectively, showing that within the available statistics, no increase of the relative contribution of photons to the gluon jet (jet 3) energy is observed.

Similarly, one can notice that the fraction of energy carried by photons relative to the total energy for events on top of the T resonance is similar (27 ± 3 %) to what is measured for events from the nearby continuum (38).

b) Number of baryons

On the contrary, a measurement of the baryon rate ($2n_{\bar{p}}/n$ charged) carried at DORIS by the DASP II collaboration (39), has shown a significant increase from the continuum (1.5 ± 1.0 %) to the T resonance (8 ± 2 %).

From a sample of 400 events with an identified $\bar{p}$, an estimate of the baryon rate in the slim and broad jet was carried out by the JADE collaboration. The values they obtained are shown in table II, together with a rough estimate of what can be expected from the DASP II result.

	Fraction of baryons in	
	slim jet	broad jet
$\langle P_\perp \rangle_{broad} > \langle P_\perp \rangle_{slim}$	45 %	55 ± 3 %
$\langle P_\perp \rangle_{broad} > 1.3 * \langle P_\perp \rangle_{slim}$	48 %	52 %
expected from T (DASP II)	38 %	63 %

Table II : baryon fraction

No significant difference between the slim and broad jet is observed, while a non zero effect might have been expected. One may remark however, beside the limited statistical significance of the above results, that baryons measured in the JADE experiment are quite soft ($.3 \lesssim p \lesssim .9$ GeV/c)^2, while the excess of baryons observed in 3 g events has been tentatively associated with leading baryon effects (24).

CONCLUSION

The neutral component of jets was analyzed in some detail for the first time ; neutral pions were observed, with an x distribution very similar to that of charged pions.

A consistent description of all phenomena observed in e^+e^- annihilation into hadrons (including correlations in rapidity, in charge and in particle angles weighted by energy) is provided by models incorporating first order QCD calculations of $q\bar{q}$ and $q\bar{q}g$ final states, followed by the fragmentation of these partons.

The Lund model seems to have some superiority over the Feynman-Field model since it reproduces better the observed differences between quark and gluon fragmentation which, although small, are significant.

An other description seems to be emerging which, relying more heavily on higher order QCD calculations, may have a chance to give a fair description of the data with simpler fragmentation models.

No difference has yet been observed between the particle content of quark and gluon jets.

ACKNOWLEDGEMENTS

I wish to thank warmly all my colleagues at PETRA whom I involved in discussions when preparing this talk. I am particularly indebted to J.F. Grivaz for careful reading and critical comments about the manuscript. Finally I thank Mrs Leloup and Mrs Mathieu for their patience with the manuscript.

FOOTNOTES

[1] The small peak around 40 MeV, reproduced by M.C. simulation, is interpreted as coming from the splitting of some γ showers into two unequal nearby showers, one giving an entry near the π° and the other one at a much lower mass.

[2] $\bar{p}(p)$ are identified using dE/dx measurements in the JADE jet chambers.

REFERENCES

(1) - W. Bartel et al., JADE Collaboration, Energy carried by gamma rays and neutral particles in multihadronic final states at PETRA, DESY 81-025.
- R. Felst, Rapporteur talk at this conference.

(2) H.J. Behrend et al., CELLO Collaboration - Comparison of the neutral and charged components of hadronic jets in e^+e^- annihilation at energies up to 36.7 GeV - Paper submitted to the EPS International Conference on High Energy Physics, (Lisbon, 1981).

(3) M. Holder, Rapporteur talk at the EPS International Conference on High Energy Physics (Lisbon, 1981).

(4) G. Wolf - private communication.

(5) - D.P. Barber et al., MARK J - Measurement of hadronic production and three jet properties at PETRA - MIT - LNS 115, July 1981.
- D.P. Barber et al., MARK J - Phys. Rep. 63 (1980) 337.

(6) P. Hoyer et al., Nucl. Phys. B161, (1979) 349.

(7) A. Ali, E. Pietarinen, G. Kramer and J. Willrodt, Phys. Lett. 93B (1980) 155.

(8) B. Anderson, G. Gustafson and C. Peterson, Z. Phys. C1 (1979) 105.
B. Anderson, G. Gustafson and T. Sjöstrand, Phys. Lett. 94B (1980) 211.
T. Sjöstrand, Lund preprint LU-TP 79-8.

(9) R.D. Field and P. Feynman, Nucl. Phys. B136 (1978) 1.

(10) Chih Kwan Chen - Why the discovery of gluons in e^+e^- annihilation is not reliable - Preprint from Purdue University, Lafayette, Indiana.

(11) R. Brandelik et al., TASSO Collaboration, Phys. Lett. 94B (1980) 444.

(12) G. Altarelli and G. Parisi, Nucl. Phys. B126 (1977) 298.

(13) B. Anderson, G. Gustafson, Z. Phys. C3 (1980) 223.
B. Anderson, G. Gustafson, T. Sjöstrand, LU-TP-80-2.
T. Sjöstrand, Lund Preprint, LU-TP-80-3.

(14) - R. Brandelik et al., TASSO Collaboration, Phys. Lett. 94B (1980) 437.
- J.E. Freeman - Direct tests of QCD in e^+e^- annihilation at PETRA - Ph. D Thesis, University of Wisconsin (1981).

(15) W. Braunschweig, Rapporteur talk at this conference.

(16) W. Bartel et al., JADE Collaboration, Phys. Lett. 101B (1981) 129.

(17) G.G. Giacomelli and M. Jacob - Physics at the CERN ISR - Phys. Rep. 55 (1979) 1.

(18) W. Koch, private communication.

(19) R. Brandelik et al., TASSO Collaboration, Phys. Lett. 100B (1981) 357.

(20) W. Bartel et al., JADE Collaboration, Phys. Lett. 104B (1981) 325.

(21) R. Brandelik et al., TASSO Collaboration, Phys. Lett. 105B (1981) 75.

(22) T. Meyer - A Monte-Carlo model to produce baryons in e^+e^- annihilations, University of Wisconsin Preprint (1981).

(23) B. Anderson, G. Gustafson, T. Sjöstrand - A model for baryon production in quark and gluon jets, Lund Preprint, LU-TP-81-3.

(24) G. Schierholz and M. Teper - Baryon production in QCD jets - DESY 81-041.

(25) - C.L. Basham et al., Phys. Rev. D19 (1979) 2018 and Phys. Rev. Lett. 41 (1978) 1585.
- L.S. Brown and S.D. Ellis - Energy correlations in e^+e^- annihilation - University of Washington Preprint - Paper submitted to the conference # 65.

(26) - K. Konishi, A. Ukawa and G. Veneziano, Phys. Lett. 80B (1979) 259.
- K. Konishi, A. Ukawa and G. Veneziano, Nucl. Phys. B157 (1979) 45.

(27) - Y.L. Dokshitzer, D.I. D'Yakonov, S.J. Troyan, Phys. Lett. 78B (1978) 280.
- G. Parisi and R. Petronzio, Nucl. Phys. B154 (1979) 427.

(28) R. Baier and K. Fey, Nucl. Phys. B179 (1981) 49.

(29) Ch. Berger et al., PLUTO Collaboration, Phys. Lett. 99B (1981) 292.

(30) A. Bassetto, private communication.

(31) R.D. Field - The production of partons and hadrons in e^+e^- annihilations, quark and gluon jet models. Invited talk at the Conference on Perturbative QCD - Tallahassee, March 1981.

(32) G.C. Fox and S. Wolfram, Nucl. Phys. B168 (1980) 225.

(33) R. Odorico, University of Bologna Preprint IFUB 80/5 (1980), to be published in Nucl. Phys. B.

(34) - J.K. Bienlein - Recent results from DORIS - Rapporteur talk at this conference.

- A. Silverman - Recent results from CESR - Rapporteur talk at this conference.

(35) A. Bassetto, M. Ciafaloni and G. Marchesini, Nucl. Phys. B163 (1980) 477.

(36) - S. Brandt and H. Dahmen, Z. Phys. C1 (1979) 61

- S.L. Wu and G. Zobernig, Z. Phys. C2 (1979) 107.

(37) C. Peterson and T.F. Walsh - Model for a nonperturbative gluon jet - Preprint NORDITA 80-1.

(38) LENA Collaboration - Paper presented to the EPS International Conference (Lisbon 1981).

(39) H. Albrecht et al., DASP II Collaboration, DESY 81-011 (1981).

Discussion

G. Barbiellini, CERN: Concerning the baryon content of gluon jets using the information from T-decay: Did you take into account the new data from CESR?

D. Fournier: No. The estimation (which in any case is very rough) is made using the data from DASP II at DORIS.

A. Engler, Carnegie-Mellon Univ.: Is there any evidence for η-production?

G. Wolf, DESY: No signal is seen in the η region, but from Monte-Carlo studies one would not expect a sizeable signal.